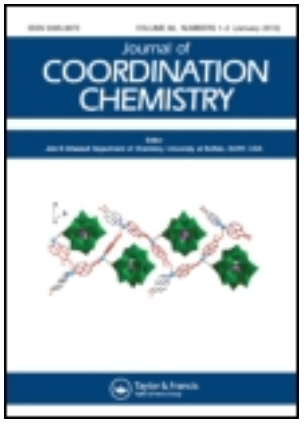

Journal of Coordination Chemistry
Publication details, including instructions for authors and subscription information:
http://www.tandfonline.com/loi/gcoo20

New self-assemblies with zinc meso-tetra[3-(1H-imidazol-1-yl)phenyl] porphyrin for use in supramolecular solar cells

Jing Cao[a], Dong-Cheng Hu[a], Jia-Cheng Liu[a], Ren-Zhi Li[b] & Neng-Zhi Jin[c]

[a] Key Laboratory of Eco-Environment-Related Polymer Materials of Ministry of Education, Key Laboratory of Polymer Materials of Gansu Province, Key Laboratory of Bioelectrochemistry & Environmental Analysis of Gansu Province, College of Chemistry and Chemical Engineering, Northwest Normal University, Lanzhou, PR China

[b] State Key Laboratory of Polymer Physics and Chemistry, Changchun Institute of Applied Chemistry, Chinese Academy of Sciences, Changchun, PR China

[c] Gansu Computing Center, Lanzhou, PR China

Published online: 04 Dec 2013.

To cite this article: Jing Cao, Dong-Cheng Hu, Jia-Cheng Liu, Ren-Zhi Li & Neng-Zhi Jin (2013) New self-assemblies with zinc meso-tetra[3-(1H-imidazol-1-yl)phenyl] porphyrin for use in supramolecular solar cells, Journal of Coordination Chemistry, 66:23, 4211-4219, DOI: 10.1080/00958972.2013.867033

To link to this article: http://dx.doi.org/10.1080/00958972.2013.867033

Journal of Coordination Chemistry, 2013
Vol. 66, No. 23, 4211–4219, http://dx.doi.org/10.1080/00958972.2013.867033

New self-assemblies with zinc *meso*-tetra[3-(1H-imidazol-1-yl) phenyl] porphyrin for use in supramolecular solar cells

JING CAO†, DONG-CHENG HU*†, JIA-CHENG LIU*†, REN-ZHI LI‡ and NENG-ZHI JIN§

†Key Laboratory of Eco-Environment-Related Polymer Materials of Ministry of Education, Key Laboratory of Polymer Materials of Gansu Province, Key Laboratory of Bioelectrochemistry & Environmental Analysis of Gansu Province, College of Chemistry and Chemical Engineering, Northwest Normal University, Lanzhou, PR China
‡State Key Laboratory of Polymer Physics and Chemistry, Changchun Institute of Applied Chemistry, Chinese Academy of Sciences, Changchun, PR China
§Gansu Computing Center, Lanzhou, PR China

(*Received 17 September 2013; accepted 14 November 2013*)

In this work, a new zinc *meso*-tetra[3-(1H-imidazol-1-yl)phenyl]porphyrin (**ZnP**) was synthesized. Further, the porphyrin **ZnP** was immobilized by metal-ligand axial coordination (**ZnP-A**) and a metal-ligand edged binding approach (**ZnP-Zn-A**) on the nanostructured TiO_2 electrode surface modified with coordinating ligand functionality, isonicotinic acid (**A**). The performances of the assemblies-sensitized solar cells were performed under irradiance of 100 mW cm^{-2} AM 1.5G sunlight. Photo-electrochemical studies reveal significantly improved performance of the assembly **ZnP-A**. These assemblies can afford a fertile base for further design and fabrication of new supramolecular solar cells in future.

Keywords: Self-assembly; Zinc porphyrin; Solar cell

1. Introduction

Dye-sensitized solar cells (DSSCs), as a cost-efficient, easy to fabrication and environmentally friendly product, have attracted considerable attention since Grätzel and co-workers cost and environmental concern,s reported their groundbreaking work on DSSCs with a porous and nano-crystalline TiO_2 electrode modified with an Ru-bipyridyl complex in 1991 [1]. Much effort has been devoted to modify the Ru(II) complexes to improve their conversion efficiencies [2–4]. However, on the basis of cost and environmental concerns, ruthenium dye is not suitable for the development of cost-efficient and environmentally friendly photovoltaic devices. In nature, photosynthetic antenna reaction centers, such as the porphyrin macrocycle as a basic chromophore framework, can use a series of intermolecular forces, such as coordination bonding, electrostatic hydrogen bonding, and weak van der

*Corresponding authors. Email: hudch@163.com (D-C Hu); jcliu8@nwnu.edu.cn (J-C Liu)

Waals interaction, to precisely tune the electronic coupling of electron donor and acceptor units in biomimetic systems [5, 6]. Inspired by this fascinating feature, porphyrin-based dyes have been used to mimic such features to construct artificial light-harvesting devices in solar cells, and the porphyrin chromophore has assured an excellent electron donor group in natural photosynthetic processes [7–12]. It is worth noting that the new PCE record of the porphyrin-based solar cell has reached 12.3% under simulated air mass 1.5 global sunlight [8]. Simultaneously, porphyrin-based self-assemblies have also attracted more attention in attempting to build artificial light-harvesting devices, with an ultimate goal of generating efficient charge separation and carrying of the separated charges to their respective electrodes in photosynthesis devices [13–16].

In our previous work, we have reported a series of new self-assemblies based on zinc porphyrin derivatives appended organic acid via a metal-ligand axial coordination and metal-ligand edged binding approach to functionalize the nanostructured TiO_2 electrode surfaces, and their respective photoelectrochemical performances were also studied [17–19]. In this work, we prepare an extension of our investigations into two new assemblies, organized by zinc *meso*-tetra[3-(1H-imidazol-1-yl)phenyl] porphyrin (**ZnP**) appended isonicotinic acid (**A**), by a metal-ligand edged binding approach (**ZnP-Zn-A**, Zn^{2+} as the metal-mediating entity) and metal-ligand axial coordination (**ZnP-A**). The detailed assembled modes are shown in scheme 1.

2. Experimental

2.1. *Materials and physical measurements*

All solvents and reagents were used directly without further purification as commercially analytical grade. Electronic absorption spectra were measured on a UV-2550 spectrometer. The luminescence spectrum was measured by a LS-55 (PE USA Inc.) fluorescence spectrophotometer at room temperature. ^{1}H NMR (400 MHz) was measured on a Varian

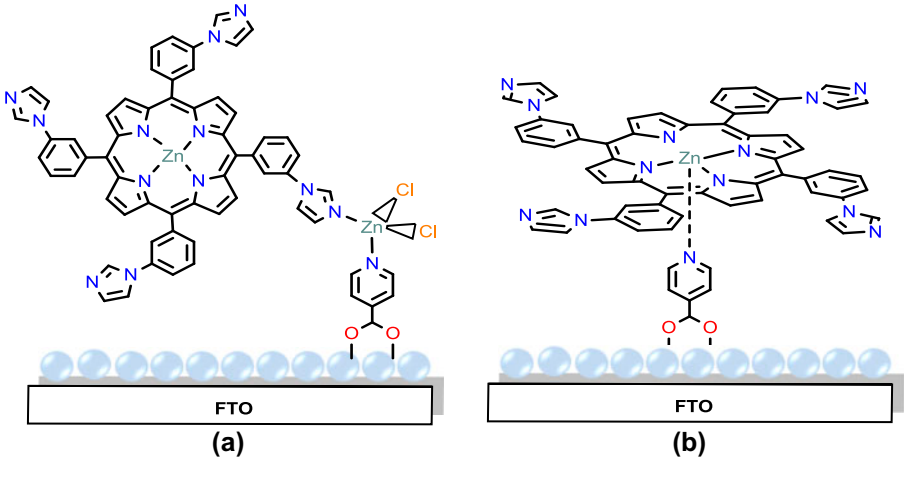

Scheme 1. The assembled modes of assemblies on TiO_2 electrode surfaces. (a) Metal-ligand edged binding approach; (b) metal-ligand axial coordination.

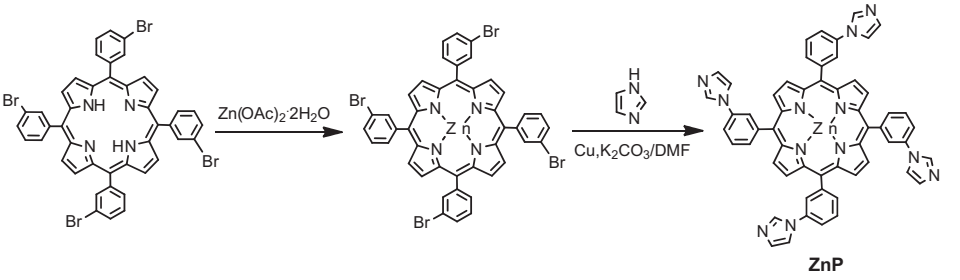

Scheme 2.

Mercury Plus-400 spectrometer. The electrospray ionization (ESI) mass spectrum was measured on a ESI-TOF mass spectrometer. The detail synthesis processes are shown in scheme 2.

2.2. *Synthesis*

5,10,15,20-tetra(*m*-bromophenyl)porphyrin was prepared according to the corresponding literature method [20]. A mixture of 5,10,15,20-tetra(*m*-bromophenyl) porphyrin (0.1 mM) and $Zn(OAc)_2{\cdot}2H_2O$ (12 mM) were dissolved in 10 mL chloroform and 2 mL methanol. The mixture was refluxed for 8 h. Then the solution was evaporated *in vacuo*. The resulting precipitate was washed by methanol solution several times. The product was collected and dried under vacuum to yield 5,10,15,20-tetra(*m*-bromophenyl)porphyrin zinc. Yield, 91%.

At the next stage, a mixture of zinc 5,10,15,20-tetra(*m*-bromophenyl)porphyrin (0.1 mM), imidazole (0.8 mM), K_2CO_3 (0.6 mM), and copper powder (0.5 mM) was added to an anhydrous DMF (10 mL), then the suspended solution was refluxed for 24 h under N_2 atmosphere (the reaction was monitored by thin-layer chromatography). After the removal of DMF, the solid was extracted with chloroform. The organic layer was dried over anhydrous sodium sulfate. The product was further purified on a silica gel column with $CHCl_3$/C_2H_5OH (1/3, v/v) as eluent to afford **ZnP**. Yield, 6.2%. ^1H NMR (400 MHz, $CDCl_3$): δ 8.89–8.91 (m, 8H, β-pyrrole), 8.74 (s, 4H, 2-imidazoyl), 8.22–8.36 (m, 8H, imidazoyl), 8.03–8.12 (m, 8H, ph), 7.72–7.78 (d, 4H, ph), 7.34–7.53 (d, 4H, ph). ESI-MS: *m/z* 940 $[M + H]^+$.

2.3. *Device Fabrication*

A screen-printed double layer film of interconnected TiO_2 particles was used as the mesoporous negative electrode. A 7 μm-thick transparent layer of 20 nm-sized titania particles were first printed on the fluorine-doped SnO_2 (FTO) conducting glass electrode and further coated by a 5 μm-thick scattering layer of 400 nm-sized titania particles. The film thickness was measured by a benchtop Ambios XP-1 stylus profilometer. The detailed preparation procedures of TiO_2 nanocrystals, pastes for screen-printing, and nanostructured TiO_2 film have been reported by Wang [21]. For the metal-ligand edged binding approach, a cycloidal TiO_2 electrode (~0.28 cm^2) was stained by immersing it into a dye solution containing i-sonicotinic acid (2 mM) as the anchoring molecule in methanol solution overnight after removal of the unbound molecules (through three ethanol washings), then immersing it into

a 2 mM $ZnCl_2$ methanol solution for 1 h, followed by washing with methanol, immersing into a dye solution containing **ZnP** (0.2 mM) in DMF for 2 h, and after this, washing by DMF solution three times. For the metal-ligand axial coordination mode, the first procedure was the same as that of the metal-ligand edged binding approach followed by immersion into a dye solution containing **ZnP** (0.2 mM) in DMF for 2 h and washing by DMF solution three times. After being washed with ethanol and dried by air flow, the sensitized titania electrode was assembled with a thermally platinized FTO electrode. The electrodes were separated by a 35 μm-thick Bynel (DuPont) hot-melt gasket and sealed up by heating. The internal space was filled with a liquid electrolyte using a vacuum backfilling system. The electrolyte-injecting hole on the counter electrode glass substrate, made with a sand-blasting drill, was sealed with a Bynel sheet and a thin glass cover by heating. The electrolyte used contained 50 mM LiI and 30 mM I_2 in acetonitrile solvent. After all these procedures, the cells were located in the oven for heating post-treatment at 100 °C for 30 min and cooled to room temperature before photoelectrochemical measurements.

2.4. *Photovoltaic Characterization*

A LS1000 solar simula-tor (Solar Light Com. Inc., USA) was used to give an irradiance of 100 mW cm^{-2} (the equivalent of one sun at AM 1.5G) at the surface of a testing cell. The current–voltage characteristics were obtained by applying external potential bias to the cell and measuring the dark current and photocurrent with a Keithley model 2602 digital source meter. This process was fully automated using Labview 8.0. A similar data acquisition system was used to control the incident photon-to-collected electron conversion efficiency (IPCE) measurement. Under full computer control, light from a 1000 W xenon lamp was focused through a monochromator onto the photovoltaic cell under test. A computer-controlled monochromator (Omni λ300) was incremented through the spectral range (300–900 nm) to generate a photocurrent action spectra with a sampling interval of 10 nm and a current sampling time of 2 s. IPCE is defined by $IPCE(\lambda) = hcJ_{sc}/e\Phi\lambda$, where h is Planck's constant, c is the speed of light in a vacuum, e is the electronic charge, λ is the wavelength (m), J_{sc} is the short-circuit photocurrent density (A m^{-2}), and Φ is the incident radiative flux (W m^{-2}). Photovoltaic performance was measured by using a metal mask with an aperture area of 0.158 cm^2. A homemade heating-cooling system was used for temperature-dependent J–V measurements.

3. Results and discussion

3.1. *UV–visible and fluorescence spectra*

The detailed data of UV–vis absorption and fluorescence spectra of **ZnP** dissolved in DMF solution (~10^{-6} M) and **ZnP-Zn-A/ZnP-A** on TiO_2 thin films are shown in table S1 (see online supplemental material at http://dx.doi.org/10.1080/00958972.2013.867033) and figure 1. The results reveal the absorption maxima in the range of 400–480 nm for strong soret (B) bands and 550–630 nm for Q bands, respectively, ascribed to π–π* transitions [22]. It can be seen that the B and Q bands of **ZnP-Zn-A/ZnP-A** are more red-shifted than those of **ZnP**, ascribed to the formation of coordination-bond of Zn-to-ligand to extend the π-conjugated system in **ZnP-Zn-A/ZnP-A**. Besides, the broadened B bands of **ZnP-Zn-A/ZnP-A** are also found, which can be ascribed to the presence of *J*-type porphyrin-aggregation on the TiO_2 surfaces [23, 24]. The considerably broadened B bands of assemblies

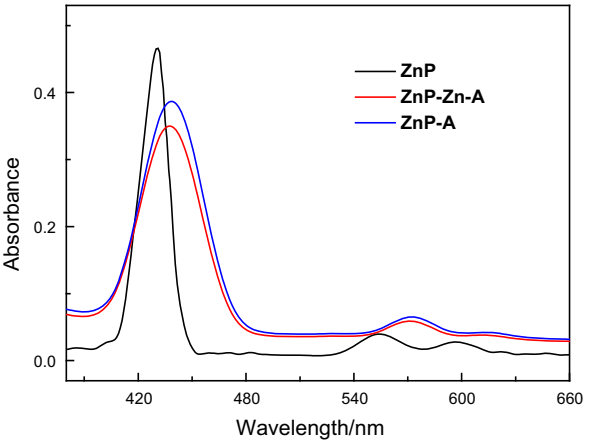

Figure 1. UV–vis spectra of **ZnP** in DMF solution and **ZnP-Zn-A/ZnP-A** on TiO_2 thin films.

indicate that the minimized gaps between the B and Q bands of the assemblies may yield significantly enhanced photoelectronic responses [25]. Notably, the absorption bands of **ZnP-A** are slightly red-shifted compared to those of **ZnP-Zn-A**, consistent with the variation of HOMO-LUMO gaps of **ZnP-A** and **ZnP-Zn-A**. As illustrated in figure 2, the results show that the emission spectrum of **ZnP** in the DMF solution is red-shifted relative to those of **ZnP-Zn-A/ZnP-A**. In addition, the emission spectra of **ZnP-A** show slight blue shifts compared to those of **ZnP-Zn-A**. These features may be ascribed to the presence of *J*-aggregation [23, 24] of porphyrin molecules on the TiO_2 surfaces, especially for the assembly **ZnP-A**.

3.2. *Molecular orbital patterns and energy levels*

To further understand the electron density distribution within the frontier and other neighboring orbitals of **ZnP-Zn-A/ZnP-A**, we performed calculations with density functional

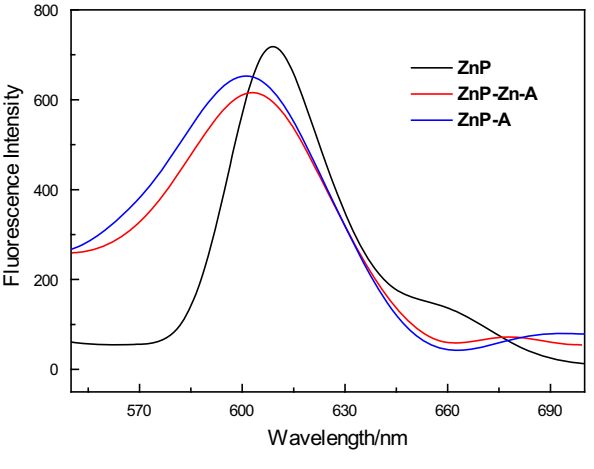

Figure 2. Fluorescence spectra of **ZnP** in DMF solution and **ZnP-Zn-A/ZnP-A** on TiO_2 thin films.

theory (DFT) using the Gaussian 09 program [26] at the B3LYP/LanL2DZ level. As shown in figure S1, the molecular orbital (MO) patterns of **ZnP-Zn-A** from HOMO-1 to LUMO+2 are consistent with those of Gouterman's four-orbital model, wherein the HOMO-1 and HOMO levels match those of the a_{1u} and a_{1u} (π) orbitals, the LUMO and LUMO+1 are similar to those of the e_g (π^*) orbitals. These features show that the electronic adsorption can be assigned to π–π^* transitions. Due to the decreased symmetry leading to minor deviation from Gouterman's four-orbital model, HOMO and LOMO levels depict partially delocalized behavior from the porphyrin center to the adjacent donor units. The electrons of LUMO+2 are concentrated at the acceptor groups, consistent with the reported results [17, 24]. However, for **ZnP-A**, the MO patterns of HOMOs are mainly localized at porphyrin cores along with slight delocalization to the adjacent donor groups. Whereas, the LUMOs display an electronic distribution on isonicotinic acid groups, indicating occurrence of excellent electron-separated status in the **ZnP-A**-sensitized device. Figure 3 shows and compares the energy-levels diagram of **ZnP-Zn-A/ZnP-A**, the valence band (VB) of TiO_2, and the electrolyte I^-/I_3^- [27]. The results show that the energy gap between the HOMO and LUMO levels is 2.83 eV for **ZnP-Zn-A** and 2.58 eV for **ZnP-A**. The LUMO levels of **ZnP-Zn-A/ZnP-A** are above that of the conducting band (CB) of TiO_2, while the HOMO levels are below the oxidation potential of electrolyte I^-/I_3^-, indicating that electrons of LUMO from the assemblies can efficiently inject the CB of TiO_2, and the excited state of the assemblies can be efficiently reduced by the electrolyte.

3.3. *Performance characterization of solar cells*

The assemblies of **ZnP-Zn-A/ZnP-A** were fabricated into DSSC devices and their respective photovoltaic behavior measured under irradiance of 100 mW cm^{-2} AM 1.5G sunlight. The photocurrent action spectra of **ZnP-Zn-A/ZnP-A**-sensitized solar cells in the wavelength range 300–800 nm are presented in figure 4. The key responses of IPCE spectra depict the energy conversion of B and Q bands of porphyrin. The features of photocurrent responses are roughly similar to their respective absorption spectra and HOMO-LUMO

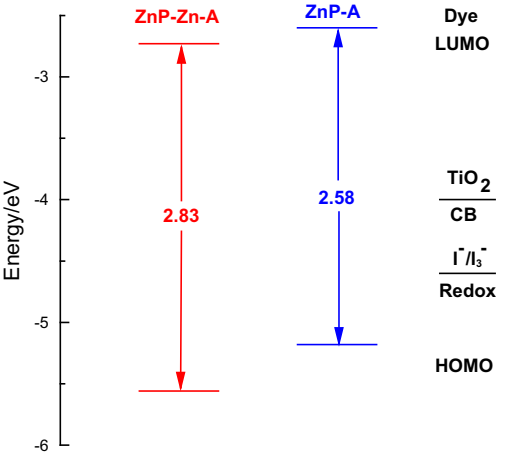

Figure 3. Orbital energy-levels of the assemblies obtained by theoretical calculation, TiO_2, and electrolyte I^-/I_3^-.

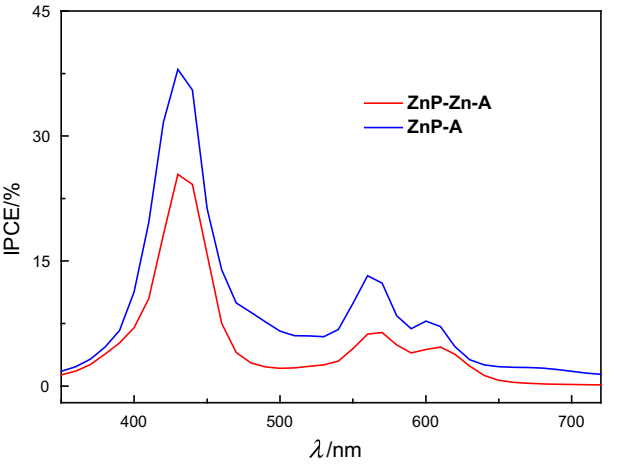

Figure 4. Photocurrent action spectra of **ZnP-Zn-A/ZnP-A**-sensitized solar cells.

gaps, especially for the broadened B bands. The maximum value of the **ZnP-A** device above 40% is significantly larger than that of the **ZnP-Zn-A** device. As shown in figure 5 and table S2, the short-circuit photocurrent density (J_{sc}), open-circuit photovoltage (V_{oc}), fill factor (FF), and overall conversion efficient (η) at AM 1.5G conditions (100 mW cm^{-2}) are 1.12 mA cm^{-2}, 0.33 V, 0.70, and 0.26% for the **ZnP-Zn-A** device; and 1.93 mA cm^{-2}, 0.30 mV, 0.67, and 0.40% for the **ZnP-A** device. The **ZnP-A** device shows a significantly enhanced conversion efficient, which could be ascribed to the formation of effective transmission channels for electron and energy transfer in the device. Besides, a larger V_{oc} is observed in the **ZnP-Zn-A** device. Notably, compared to our previous reported assemblies (**ZnP1-A**) based on zinc *meso*-tetra[4-(1H-imidazol-1-yl)phenyl]porphyrin (**ZnP1**) [17], the **ZnP-A** device reveals enhanced photovoltaic properties under the same assembled and

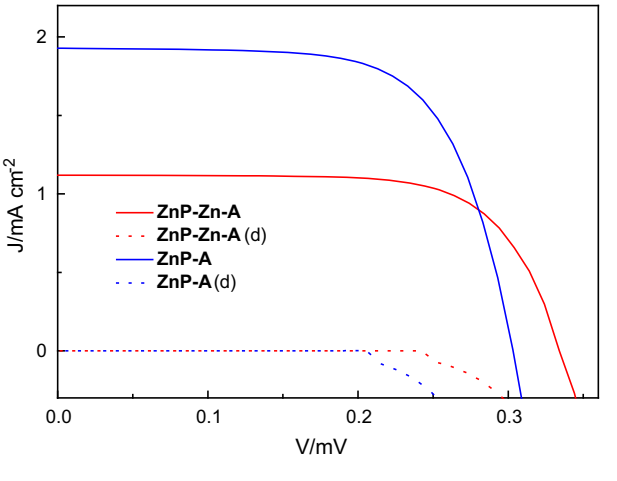

Figure 5. *J-V* characteristics of **ZnP-Zn-A/ZnP-A**-sensitized SC measured under irradiance of 100 mW cm^{-2} AM 1.5G sunlight (**ZnP-Zn-A/ZnP-A**) and in the dark (**ZnP-Zn-A/ZnP-A**(d)).

measured conditions (figures S2, S3 and table S2), but, it is worse than other acetohydrazide Zn(II) porphyrin devices reported in our previous work [18, 19]. The lower overall performances of ZnPx-A-sensitized cells reported in this article can be mainly assigned to the small amount of adsorbed porphyrin-sensitizers on TiO_2 electrode surfaces to capture the inefficient light harvesting, reflected by the faint color of sensitized electrodes and the low UV–vis absorbing properties.

4. Conclusions

In summary, we have successfully synthesized and characterized two new self-assemblies (**ZnP-Zn-A** and **ZnP-A**) based on zinc *meso*-tetra[3-(1H-imidazol-1-yl)phenyl]porphyrin (**ZnP**) appended isonicotinic acid ligands (**A**) by metal-ligand axial coordination and a metal-ligand edged binding approach. Photo-electrochemical studies reveal that the assembly **ZnP-A** shows a significantly improved photocurrent response, which also outperforms the performance of our previous reported assembly with zinc *meso*-tetra[4-(1H-imidazol-1-yl) phenyl]porphyrin under the same conditions. However, compared with other reported sensitizers of polymeric metal complexes containing 8-hydroxyquinoline [28], although the values of their V_{oc} are larger than that of **ZnP-A**, a significantly enhanced J_{sc} is observed for **ZnP-A**. This work affords a fertile base for further investigation into supramolecular solar cells.

Acknowledgements

We are very grateful to Prof. Peng Wang (Changchun Institute of Applied Chemistry, Chinese Academy of Sciences) for supplying device fabrication and measurement of solar cells. We also thank the support of Gansu Computing Center of China.

Funding

This work was supported by the National Natural Science Foundation of China [grant number 20871099]; Gansu provincial Natural Science Foundation of China [grant number 0710RJZA113].

References

[1] B. Oregan, M. Grätzel. *Nature*, **353**, 737 (1991).
[2] S.M. Zakeeruddin, M. Grätzel. *Adv. Funct. Mater.*, **19**, 1 (2009).
[3] Y.M. Cao, Y. Bai, Q.J. Yu, Y.M. Cheng, S. Liu, D. Shi, F.F. Gao, P. Wang. *J. Phys. Chem. C*, **113**, 6290 (2009).
[4] C. Sahin, C. VarlikII, C. Zafer, Q. Shi, R.E. Douthwaite. *J. Coord. Chem.*, **66**, 1384 (2013).
[5] J. Deisenhofer, O. Epp, K. Miki, R. Huber, H. Michel. *Nature*, **318**, 618 (1985).
[6] J. Deisenhofer, O. Epp, K. Miki, R. Huber, H. Michel. *J. Mol. Biol.*, **180**, 385 (1984).
[7] K.M. Smith. *Porphyrins and Metalloporphyrins*., Elsevier, Amsterdam (1972).
[8] A. Yella, H.W. Lee, H.N. Tsao, C. Yi, A.K. Chandiran, M.K. Nazeeruddin, E.W.G. Diau, C.Y. Yeh, S.M. Zakeeruddin, M. Grätzel. *Science*, **334**, 629 (2011).
[9] W.M. Campbell, A.K. Burrell, D.L. Officer, K.W. Jolley. *Coord. Chem. Rev*, **248**, 1363 (2004).
[10] T. Ichiki, Y. Matsuo, E. Nakamura. *Chem. Commun.*, **49**, 279 (2013).
[11] M.E. Milanesio, M. Gervaldo, L.A. Otero, L. Sereno, J.J. Silber, E.N. Durantini. *J. Phys. Org. Chem.*, **15**, 844 (2002).
[12] O. Ito, F. D'Souza. *Molecules*, **17**, 5816 (2012).

[13] N.K. Subbaiyan, C.A. Wijesinghe, F. D'Souza. *J. Am. Chem. Soc.*, **131**, 14646 (2009).
[14] A. Kira, T. Umeyama, Y. Matano, K. Yoshida, S. Isoda, J.K. Park, D. Kim, H. Imahori. *J. Am. Chem. Soc.*, **131**, 3198 (2009).
[15] C.M. Drain, F. Nifiatis, A. Vasenko, J.D. Batteas. *Angew. Chem. Int. Ed.*, **37**, 2344 (1998).
[16] D.J. Qian, C. Nakamura, T. Ishida, S.O. Wenk, T. Wakayama, S. Takeda, J. Miyake. *Langmuir*, **18**, 10237 (2002).
[17] J. Cao, J.C. Liu, W.T. Deng, R.Z. Li, N.Z. Jin. *Org. Electron.*, **14**, 2713 (2013).
[18] J. Cao, J.C. Liu, W.T. Deng, R.Z. Li, N.Z. Jin. *Electrochim. Acta*, **112**, 515 (2013).
[19] J. Cao, J.C. Liu, L.W. Chen, R.Z. Li, N.Z. Jin. *Tetrahedron Lett.*, **54**, 3851 (2013).
[20] C.A. Hunter, M.C. Misuraca, S.M. Turega. *J. Am. Chem. Soc.*, **133**, 582 (2011).
[21] P. Wang, S.M. Zakeeruddin, P. Comte, R. Charvet, R. Humphry-Baker, M.E. Grätzel. *J. Phys. Chem. B*, **107**, 14336 (2003).
[22] M. Gouterman. *J. Mol. Spectrosc.*, **6**, 138 (1961).
[23] C. Yang, Z.M. Yang, H.W. Gu, C.K. Chang, P. Gao, B. Xu. *Chem. Mater.*, **20**, 7514 (2008).
[24] C.Y. Lin, C.F. Lo, L.Y. Luo, H.P. Lu, C.S. Hung, E.W.G. Diau. *J. Phys. Chem. C*, **113**, 755 (2009).
[25] C.Y. Lin, Y.C. Wang, S.J. Hsu, C.F. Lo, E.W.G. Diau. *J. Phys. Chem. C*, **114**, 687 (2010).
[26] M.J. Frisch, G.W. Trucks, H.B. Schlegel, G.E. Scuseria, M.A. Robb, J.R. Cheeseman, G. Scalmani, V. Barone, B. Mennucci, G.A. Petersson, et al., *Gaussian 09, Revision A. 02, Gaussian, Inc.* Wallingford, CT, USA, (2009).
[27] R.Z. Li, X.J. Lv, D. Shi, D.F. Zhou, Y.M. Cheng, G.L. Zhang, P. Wang. *J. Phys. Chem. C*, **113**, 7469 (2009).
[28] L.R. Zhanga, G.J. Wena, Q. Xiua, L.H. Guoa, J.Y. Denga, C.F. Zhong. *J. Coord. Chem.*, **65**, 1632 (2012).